Energy Proceedings
Vol 46, 2024
ISSN 2004-2965

Three-dimensional numerical investigation on the transient response characteristics of DIR-SOFC during increasing electrical load process

Bohan Li, Chaoyang Wang*, Junjie Yan

State Key Laboratory of Multiphase Flow in Power Engineering, Xi'an Jiaotong University, Xi'an 710049, China

(Corresponding author: Chaoyang Wang*

Email: chaoyang.wang@xjtu.edu.cn)

ABSTRACT

Solid oxide fuel cell (SOFC) is a promising power technology with clean, high efficiency, and exceptionally high fuel flexibility. This research established and experimentally verified a 3D-dynamic model of a planar direct internal reforming (DIR) SOFC. Based on the developed model, the 500-second dynamic response characteristics of the cell fueled by pure hydrogen or 0.3 pre-reformed syngas were investigated after increasing the power density by 20%. The results show that the power density response of the cell, whether hydrogen or syngas-fueled, can be divided into a concentration-dominated fast-response stage with a subsequent temperature-dominated slow-response stage. The fast-response stage is finished in a few seconds, while the slow-response stage takes hundreds of seconds to stabilize. When the initial power density (P_0) is relatively low (P_0=1500W/m^2), the changes in the fast-response stage account for more than 93% of the whole process, indicating that the power density can be stabilized quickly. As the initial power density increases, the proportion of power density change in the slow-response stage gradually increases and reaches more than 50%. When P_0=4000W/m^2, the power density of the cell fueled by hydrogen or syngas increases by 400 W/m^2 and 520 W/m^2, respectively, in the slow-response stage, corresponding to 50% and 65% of the whole process.

Keywords: Solid oxide fuel cell, 3D dynamic model, transient performance, direct internal reforming, DIR-SOFC

NONMENCLATURE

Abbreviations	
RES	Renewable Energy Sources
SOFC	Solid oxide fuel cell
DIR	Direct internal reforming
CCL	Current collection layers
Symbols	
τ	Times
P_0	Initial power density

1. INTRODUCTION

To attain net-zero emissions by mid-century, carbon neutrality necessitates a rapid transition from fossil fuels to Renewable Energy Sources (RES) [1]. The power generation from RES has grown exponentially in recent years, but the stochastic and intermittent characteristics of RES pose various problems and challenges, such as grid congestion, grid frequency deviation, and difficulty in coordinating the operational schedules of conventional power plants [2]. These phenomena highlight the importance of developing and implementing energy storage technologies [3]. Among various energy storage and power generation technologies, hydrogen storage and conversion system based on direct internal reforming solid oxide fuel cells (DIR-SOFC) have remarkable attributes, such as high conversion efficiency, clean emission, and wide fuel flexibility [4]. When a SOFC-based energy storage system is integrated with RES, the unpredictability of RES and the time-varying electricity demand high flexibility in the energy storage system for keeping the frequency of the power system within a tolerable range [5]. As the key component of the energy storage system, SOFC has to switch between different output powers frequently and rapidly. To improve the SOFC system's flexibility and develop reasonable control strategies, it is essential to understand the dynamic response characteristics of SOFC during the increasing electrical load process.

In recent years, many studies have been conducted on the transient processes and performance of SOFC. The transient responses of current density, cell temperature, and reactant concentration to the loading output voltage under various operating conditions were examined by Yuan et al. [6]. Ho [7] showed the temporal profiles of temperature, activated overpotential, and gas concentration distribution in the cell following a sudden

This is a paper for 15th International Conference on Applied Energy (ICAE2023), Dec. 3-7, 2023, Doha, Qatar.

change in output voltage from 0.7V to 0.6V or 0.8V. Wang et al. [8] investigated the effects of stack design and operating parameters, such as stack heat capacity, operating pressure, and fuel composition, on the mode-switching process. Fogel et al. [9] developed a 2D dynamic model of a single tubular SOEC to simulate its transient behaviors during fast load changes at different switching rates. Nerat [10] created a 3D dynamic model of a single SOFC channel by using COMSOL Multiphysics and explored the evolution of local mass fractions of fuel species after a step change in output voltage. The dynamic responses of the average current density during the heat up, start up, and load changing phases for both counterflow and co-flow configurations of DIR-SOFC were evaluated by Choudhury et al. [11].

The above literature review illustrates that the transient processes of SOFC have been studied widely. However, most of these studies only considered the input-output relationship based on 0D or 1D models and neglected the internal behaviors of SOFC. To address this research gap and examine the possibility of enhancing the flexibility of SOFC, a high-resolution 3D single-cell dynamic model of a co-flow planar SOFC is established in the COMSOL Multiphysics software. Based on the developed model, the 500-second dynamic response characteristics of the cell fueled by pure hydrogen or 0.3 pre-reformed syngas were investigated after increasing the power density by 20%. The results obtained in this research can provide theoretical guidance for the actual operation of the cell and lay the foundation for designing new system dynamic control strategies.

2. NUMERICAL SIMULATION

2.1 Geometry and mathematical models

As shown in *Fig. 1* (a), repeated single-cell units constitute the SOFC stack, each comprising top and bottom interconnects, gas flow channels, Ni and Pt meshes, and a sandwich-structured SOFC cell. The Ni-foam and Pt-mesh are assumed to be inserted into the cell and interconnects as the current collection layers (CCL) to enhance the current collection. The gases flow in the same direction through the interleaved air and fuel electrode channels. The cell is symmetrically simplified to improve computational efficiency. Fig. 1 (b) and (c) display the simplified schematic diagram of a repeated single-cell unit and the illustration for the configuration of the sandwich-structured SOFC cell, respectively. The thickness of different layers and other geometric parameters can be found in our past research [12].

The main assumptions involved in the modeling process are as follows: (a) All the gases involved in the model are considered to be ideal gases; (b) Porous electrodes are isotropic and homogeneous permeable; (c) A laminal flow model is used to calculate the gas flow due to the low Reynolds number; (d) Only the radiation

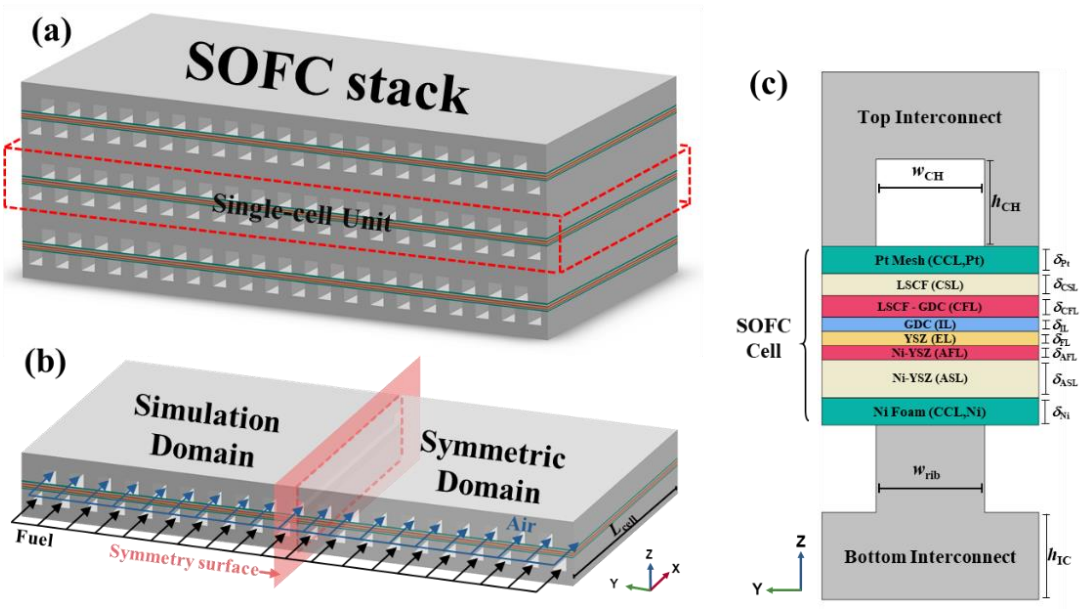

Fig. 1 Schematic illustration for (a) configuration of a planer SOFC stack, (b) a repeated single-cell unit, and (c) sandwich-structured SOFC cell

heat transfer between the outer surface and environment is considered, and the other types of radiation heat transfer are ignored. Further details, including the governing equations, chemical reaction kinetics model, corresponding constitutive equations, materials, and fluid parameters, can be found in [13-15].

2.2 boundary conditions

Appropriate initial and boundary conditions are the basis for numerical calculations. The anode interconnector's bottom surface is set to zero potential and the cathode interconnector's top surface is set to U_{cell}. The other external boundaries are thermally insulated. The cell operates at 1023K. The anode and cathode receive preheated fuel and air, respectively. The fuel used in the cell is hydrogen and 30% pre-reformed syngas, respectively, with fuel molar ratios of 26.3% H_2, 49.3% H_2O, 17.1% CH_4, 2.94% CO and 4.36% CO_2 [16]. The outlet of the working fluid has convection boundary conditions, and the ambient pressure is set to the atmospheric pressure (1 atm). *Table 1* shows more details about the boundary conditions for various surfaces.

2.3 Model validation

Commercial software COMSOL Multiphysics 6.0 is used to numerically solve the governing equations of the thermodynamic, mass transport, and thermal models. Two consecutive simulations are performed to solve the fully coupled, dynamic, and nonlinear conservation equations. The steady-state process was first calculated, and then the initial steady result was used as the initial condition for the following time-dependent simulation of the transient response process. The simulated and experimental current densities for both steady-state and transient conditions were compared to verify the model's reliability. The experimental data were obtained from Lee et al. [17] and Bae et al. [18], who measured the steady-state performance curves of SOFC at different temperatures and the transient response of the current density for a voltage step change, respectively. *Fig. 2* (a) and (b) show the comparison results, which indicate that the model developed in this work is reliable, as the relative error is less than 2% for both cases.

Table 1 Boundary conditions used in the DIR-SOFC model

Boundary	Boundary conditions			
	Momentum	Thermal	Species	Electric potential
Top interconnect surface	Stationary wall and no slip	Symmetry	Zero diffusive flux	$\Phi_{top} = U_{cell}$
Bottom interconnect surface	Stationary wall and no slip	Symmetry	Zero diffusive flux	$\Phi_{bottem} = 0$
Air inlet	Q_{sccm} = 30 SCCM	T = 1023K	$x_{O_2} = 0.21$ $x_{N_2} = 0.79$	insulation
Air outlet	P = 1 atm	Convection	Convection	insulation
Fuel inlet	Q_{sccm} = 7 SCCM	T = 1023K	Hydrogen / 30% pre-reformed syngas	insulation
Fuel outlet	P = 1 atm	Convection	Convection	insulation
Front and back walls	Stationary wall and no slip	Surface to environment radiation, ε = 0.6	Zero diffusive flux	insulation

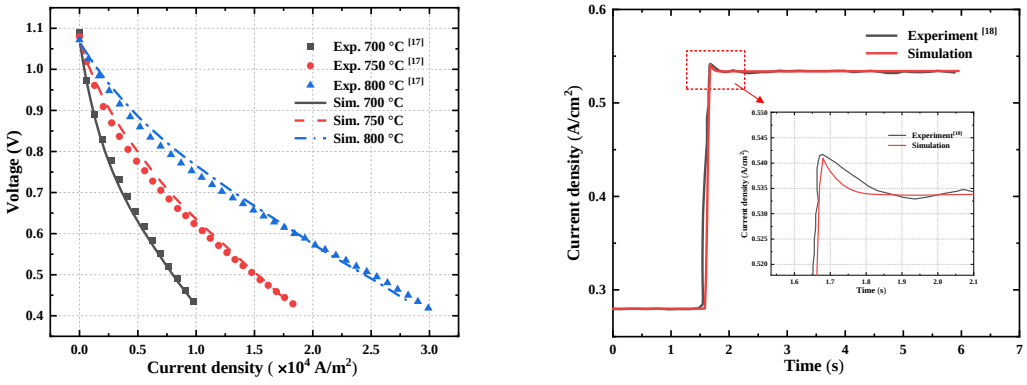

(a) (b)

Fig. 2 Validations of the proposed dynamic SOFC model for (a) steady-state performance curves of SOFC and (b) the transient response of the current density after a step change in the electric potential from 0.8 V to 0.6 V

3. RESULTS AND DISCUSSIONS

In this study, we investigated the 500-second dynamic response characteristics of DIR-SOFC fueled by pure hydrogen or 0.3 pre-reformed syngas after increasing the power density by 20%. The investigated SOFC dynamic process can be described specifically as follows.

1) During τ=1-10s, the cell operates at a steady state. The initial power density (P_0) is 1500W/m^2 and 4000W/m^2, respectively.

2) At τ=10s, the output voltage of the cell changes within a short time of 0.1s and stays constant for the rest of the dynamic response process. The power density increases by 20% due to the change in the output voltage.

3) After improving the output voltage, the dynamic response of SOFC is simulated until τ=500s, at which point the cell attains a new steady state.

3.1 Dynamic response characteristics of SOFC when P_0 = 1500W/m^2

The cells fueled by different fuels have different steady performances as shown in *Fig. 3*. It can be observed that the the current density of hydrogen-fueled SOFC is higher than that of syngas-fueled SOFC for the same output voltage. The maximum power densities for hydrogen-fueled and syngas-fueled SOFC are 6390W/m^2 and 5040W/m^2, respectively. The reason for this phenomenon is that methane in syngas-fueled SOFCs needs to be converted to hydrogen through a series of complex chemical reactions, and therefore the hydrogen concentration inside the porous electrodes is relatively low.

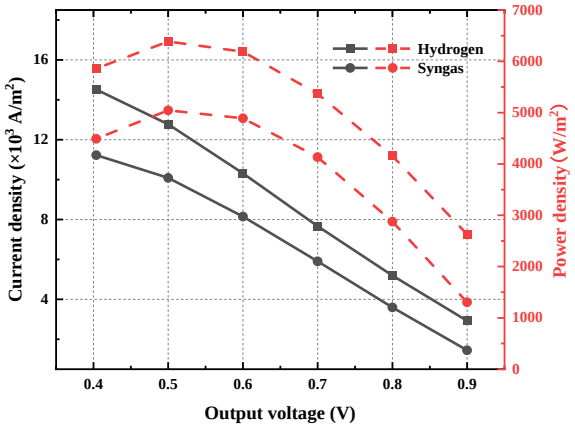

Fig. 3 Steady power density- versus output voltage of SOFC fueled by pure hydrogen or 0.3 pre-reformed syngas

The dynamic response characteristics of SOFC are different as the initial power density varies. *Fig. 4* illustrates the dynamic response process for a 20% increase in power density when P_0=1500W/m^2. Notably, the response process can be divided into fast-response and slow-response stages. Taking the response process of hydrogen-fueled SOFC as an example, the power density sharply rises by 285W/m^2 (19%) during τ=10-11s but only rises by less than 1% in the following 200s. This is because mechanisms of increasing the power density are different in these two stages. During the first fast-rising stage, the increased concentration of the reactants within the functional layers is the main reason causing the power density increase. The higher current density then generates excessive heat, causing a constant rise in the cell temperature. In the following second slow-rising stage, the improvement in the output power density can be attributed to the continuous increase in the cell temperature. The higher temperature improves the cell's performance and thus increases the power density.

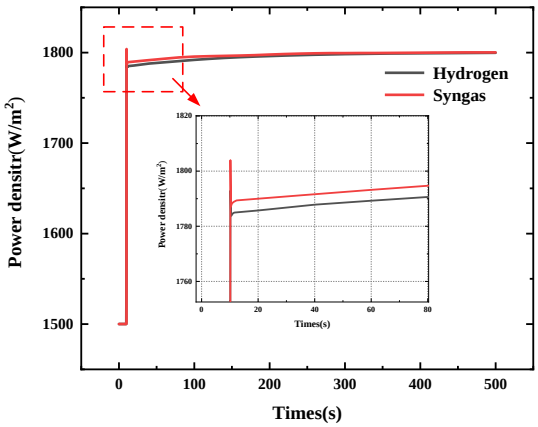

Fig. 4 The dynamic response process for a 20% increase in power density when P_0=1500W/m^2

Fig. 5 shows the evolution of the average temperature of the functional layers during the dynamic response process when P_0=1500W/m^2. It can be observed that the temperature difference of the functional layers is less than 1K. This small temperature difference results in an insignificant increase in the output power density (15W/m^2) of the cell during τ = 11-200s. Under this situation, the power regulating transient process can be completed within a very short time.

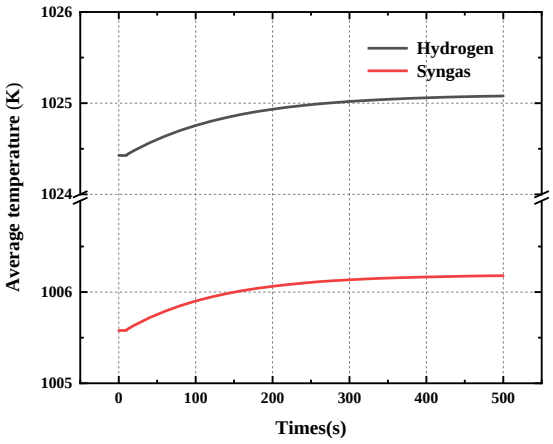

Fig. 5 Temporal evolution of average temperature of SOFC's functional layers during the dynamic response process when P_0=1500W/m^2

3.2 Dynamic response characteristics of SOFC when P_0 = 4000W/m^2

As the initial power density increases, the proportion of power density change in the slow-response stage gradually increases. *Fig. 6* illustrates the dynamic response process for a 20% increase in power density when P_0=4000W/m^2. The power density of the cell fueled by hydrogen or syngas increases by 400 W/m^2 and 520 W/m^2 respectively in the slow-response stage, corresponding to 50% and 65% of the whole response process. It can be found that when P_0 is high, the temperature-dominated slow-response stage becomes the main part of the whole response process due to the significant cell temperature change before and after the transient process. In this case, the transient response process for power changes needs to take hundreds of seconds to stabilize.

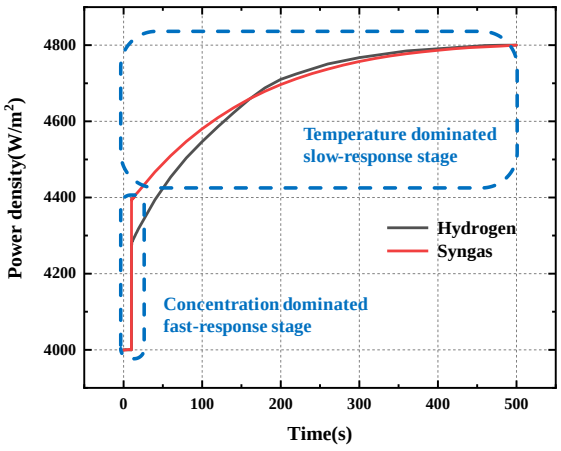

Fig. 6 The dynamic response process for a 20% increase in power density when P_0=4000W/m^2

Fig. 7 illustrates the evolution of the average temperature of the functional layers during the dynamic response process when P_0=4000W/m^2. The difference in temperature before and after the transient process for hydrogen-fueled and syngas-fueled SOFCs are 7 K and 10 K, respectively. After increasing the same power density, the current density of the syngas-fueled SOFC increases by 2150 A/m^2, while the current density of the syngas-fueled SOFC increases by 1558 A/m^2. It can be seen that the current density of the syngas-fueled SOFC increases more dramatically, and the resulting thermal effect is more pronounced. As a result, the cell temperature of the syngas-fueled SOFC increases more. Due to the considerable temperature increase, the slow-response stage of syngas-fueled SOFC accounts for a higher proportion of the whole transient process than hydrogen-fueled SOFC, as shown in *Fig. 6*. The results of this study show that reducing the temperature change of the cell to reduce the power density transient response time and thus improve the SOFC-based system regulation flexibility is a promising approach.

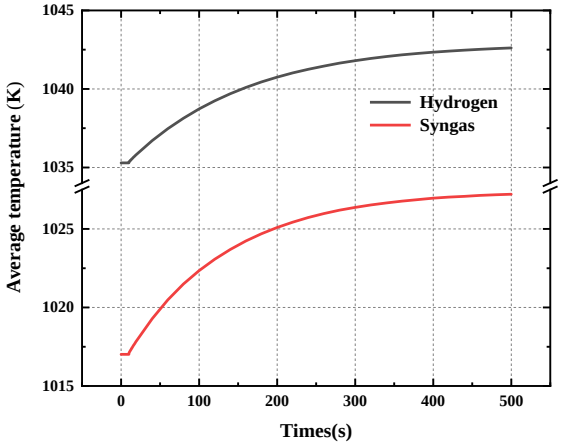

Fig. 7 Temporal evolution of average temperature of SOFC's functional layers during the dynamic response process when P_0=4000W/m^2

4. CONCLUSIONS

This study establishes a 3D dynamic model of a solid oxide fuel cell to investigate the dynamic response characteristics of DIR-SOFC fueled by pure hydrogen or 0.3 pre-reformed syngas after increasing the power density by 20%. This study's results show that the cell's power density response, whether hydrogen or natural gas-fueled, can be divided into a concentration-dominated fast-response stage with a following temperature-dominated slow-response stage. The increased concentration of reactants within the porous electrodes is the main reason causing the power density

increase in the first fast-response stage. In the following slow-response stage, the improvement in the power density can be attributed to the continuous increase in the cell temperature. The fast-response stage accounts for more than 90% of the total transient response process when the initial power density is relatively low. As the initial power density increases, the proportion of the slow-response stage gradually increases and reaches more than 50%. When P_0=4000 W/m^2, the power density of the cell fueled by hydrogen or syngas increases by 400 W/m^2 and 520 W/m^2, respectively, in the slow-response stage, corresponding to 50% and 65% of the whole process.

ACKNOWLEDGEMENT

This work was supported by the National Natural Science Foundation of China (Grant Number 52106026), the Fundamental Research Funds for the Central Universities (Grant Number xzy012021012), and Natural Science Basic Research Program of Shaanxi (Program No. 2021JLM-34).

REFERENCE

[1] Gür TM. Review of electrical energy storage technologies, materials and systems: challenges and prospects for large-scale grid storage. Energy & Environmental Science. 2018;11(10):2696-767.
[2] Cherp A, Vinichenko V, Tosun J, Gordon JA, Jewell J. National growth dynamics of wind and solar power compared to the growth required for global climate targets. Nature Energy. 2021;6(7):742-54.
[3] Guerra OJ, Eichman J, Denholm P. Optimal energy storage portfolio for high and ultrahigh carbon-free and renewable power systems. Energy & Environmental Science. 2021;14(10):5132-46.
[4] Olabi AG, Onumaegbu C, Wilberforce T, Ramadan M, Abdelkareem MA, Al – Alami AH. Critical review of energy storage systems. Energy. 2021;214.
[5] Aneke M, Wang M. Energy storage technologies and real life applications – A state of the art review. Applied Energy. 2016;179:350-77.
[6] Yuan P, Liu S-F. Transient analysis of a solid oxide fuel cell unit with reforming and water-shift reaction and the building of neural network model for rapid prediction in electrical and thermal performance. International Journal of Hydrogen Energy. 2020;45(1):924-36.
[7] Ho TX. Dynamic characteristics of a solid oxide fuel cell with direct internal reforming of methane. Energy Conversion and Management. 2016;113:44-51.
[8] Wang C, Chen M, Liu M, Yan J. Dynamic modeling and parameter analysis study on reversible solid oxide cells during mode switching transient processes. Applied Energy. 2020;263.
[9] Fogel S, Kryk H, Hampel U. Simulation of the transient behavior of tubular solid oxide electrolyzer cells under fast load variations. International Journal of Hydrogen Energy. 2019;44(18):9188-202.
[10] Nerat M. Modeling and analysis of short-period transient response of a single, planar, anode supported, solid oxide fuel cell during load variations. Energy. 2017.
[11] Choudhary T, Sanjay. Computational analysis of IR-SOFC: Transient, thermal stress, carbon deposition and flow dependency. International Journal of Hydrogen Energy. 2016;41(24):10212-27.
[12] Li B, Wang C, Liu M, Yan J. Numerical investigation of the transient performance of a reversible solid oxide cell during the mode switching process. Energy Conversion and Management. 2022;268.
[13] Haberman BA, Young JB. Three-dimensional simulation of chemically reacting gas flows in the porous support structure of an integrated-planar solid oxide fuel cell. International Journal of Heat and Mass Transfer. 2004;47(17-18):3617-29.
[14] Li B, Wang C, Liu M, Fan J, Yan J. Transient performance analysis of a solid oxide fuel cell during power regulations with different control strategies based on a 3D dynamic model. Renewable Energy. 2023;218.
[15] Gokon N, Osawa Y, Nakazawa D, Kodama T. Kinetics of CO2 reforming of methane by catalytically activated metallic foam absorber for solar receiver-reactors. International Journal of Hydrogen Energy. 2009;34(4):1787-800.
[16] Li Z, Yang G, Cui D, Li S, Shen Q, Zhang G, et al. Modeling and evaluating of thermo-electro-chemo-mechanical behavior for pre-reformed methane-fueled solid oxide fuel cell. Journal of Power Sources. 2022;522.
[17] Lee S, Kim H, Yoon KJ, Son J-W, Lee J-H, Kim B-K, et al. The effect of fuel utilization on heat and mass transfer within solid oxide fuel cells examined by three-dimensional numerical simulations. International Journal of Heat and Mass Transfer. 2016;97:77-93.
[18] Bae Y, Lee S, Yoon KJ, Lee J-H, Hong J. Three-dimensional dynamic modeling and transport analysis of solid oxide fuel cells under electrical load change. Energy Conversion and Management. 2018;165:405-18.